WCCAP Report

Absorption Photometer Workshop

Thomas Müller, Alfred Wiedensohler, Thomas Tuch et. al

Leibniz Institute for Tropospheric Research, Leipzig, Germany

1 Introduction

The first absorption photometer workshop was held in Leipzig at the Leibniz Institute for Tropospheric Research, November 2005. This report summarizes results of the intercomparions, which will be published together with the results of the second workshop held in March 2007.

1.1 Background

Spectral aerosol light absorption is an important parameter for the assessment of the radiation budget of the atmosphere. Although on-line measurement techniques for aerosol light absorption, such as the Aethalometer, the Particle Soot Absorption Photometer (PSAP), and the Multi Angle Absorption Photometer (MAAP) have been available for several years, they are limited in accuracy and spectral resolution because of the need to deposit the aerosol on a filter substrate before measurement. The commercial single-wavelength PSAP was modified to measure at three wavelengths (Virkkula, 2005). A 7-wavelength Aethalometer became commercially available, which covers the visible (UV/VIS) to near-infrared (NIR) spectral range (λ=370–950 nm). However, the applicability of the laboratory calibration factors to ambient conditions is still not well understood. A recently presented calibration for Aethalometer (Schmid 2006) using ambient aerosol differs by a factor of 1.3 from a calibration using laboratory aerosols (Weingartner 2003).

A limiting factor for all filter based absorption photometers is the cross sensitivity to particle scattering. Furthermore a loading dependent calibration factor complicates the evaluation of a calibration function. In the last years several correction schemes were developed for different types of instruments. A description of these methods is given in chapter 2.1.

1.2 Goals of the inter-comparison workshop

The different correction schemes for the instruments and the unit to unit variability within a class of instruments complicates an inter-comparison of different instruments. To overcome the problem of unit to unit variability several instruments of one type are needed. An inter-comparison between instrument classes strongly depends of the method of correction which is applied. The goals of the absorption photometer work-

shop are to compare different instruments taking into account the instrument variability. The specific goals are:

a) to determine the unit to unit variability of instruments,

b) to determine the relative sensitivities of the different instruments types to absorbing and scattering particles,

c) to find parameters, which affect the accuracy of instruments.

During the workshop several experiments were done which were dedicated to achieve the specific goals. Different types of aerosols were used.

A brief overview of the workshop is given in the following chapters. A description of the experimental setup including the instruments and the aerosol generation is given in Chapter 2. In Chapter 3 a characterization of the instruments is given. The results of the inter-comparison are given in Chapter 4, and a discussion follows in Chapter 5.

1.3 Organization

The workshop was held at the Leibniz Institute for Tropospheric Research (IfT) in Leipzig from 13 to 17 November, 2005. IfT provides several laboratories for the workshop. The laboratories were equipped with the aerosol generators and systems for a basic aerosol characterization.

A total of 24 participants attended the workshop with 24 systems for measuring the particle absorption. A summary of all absorption photometers is given in Table 1.2. In total nine PSAP (Radiance Research) and 2 custom made PSAPs were compared during the workshop. Furthermore seven MAAPs, six Aethalometers, a SOAP (spectral, optical absorption photometer) and a PAS were used during the workshop.

Table 1.1: List of participants

Name	Institution	Identification
Alfred Wiedensohler	Leibniz Institute for Tropospheric Research	IFT
Thomas Tuch	Leibniz Institute for Tropospheric Research	IFT
Thomas Müller	Leibniz Institute for Tropospheric Research	IFT
Brendan Kelly	Atmospheric Research Group, Physics Department, NUI Galway.	MHD
Mathieu Fricker	Deutscher Wetterdienst, Medizin Meteorologie Freiburg	DWD
Friedhelm Welz	Deutscher Wetterdienst, Medizin Meteorologie Freiburg	DWD
Andreas Petzold	Deutsches Zentrum für Luft- und Raumfahrt	DLR
Jan Hasselbach	Deutsches Zentrum für Luft- und Raumfahrt	DLR
Sergio Rodriguez	Izana Atmospheric Observatory	IZANA
Uwe Kaminski	Meteorologisches Observatorium, DWD, GAW Global Station	DWD
Reinhard T. Wilhelm	Meteorologisches Observatorium, DWD, GAW Global Station	DWD
Erik Engström	Department of Meteorology, Stockholm University	MISU
Aki Virkkula	Finnish Meteorological Institute	FMI
Ng Chee Wah	Malaysian Meteorological Service	MMS
John Ogren	NOAA Earth System Research Laboratory / GMD	NOAA
Nikos Kalivitis	Environmental Chemical Processes Laboratory, University of Crete	ECPL
Günther Wehrle	Paul Scherrer Institut, Department of Atmospheric Chemistry	PSI
Ernest Weingartner	Paul Scherrer Institut, Department of Atmospheric Chemistry	PSI
Aniko H. Veres	University of Szeged, Department of Optics and Quantum Electronics	USZ
Arpad Mohacsi	University of Szeged, Department of Optics and Quantum Electronics	USZ
Antti Hyvärinen	Finnish Meteorological Institute	FMI
Junying Sun	Centre for Atmosphere Watch and Services, Chinese Academy of Meteorological Sciences	CAWAS

Table 1.2: Overview of instruments and instrument IDs

Instrument Type	**Serial Number**	**Institution**	**Instrument ID**
PSAP	48	ECPL	ECPL 48
PSAP 3λ	90A	FMI	FMI 90A
PSAP	20A	IFT	IFT 20A
PSAP	20B	IFT	IFT 20B
PSAP	71	IFT	IFT 71
PSAP 3λ	90B	NOAA	NOAA 90B
PSAP	13	NOAA	NOAA 13
PSAP	MISU	MISU	MISU
PSAP	ITM	ITM	ITM
PAS 3λ		USZ	
Spectral Optical Absorption Photometer		IFT	SOAP
AETH 7λ, AE31	483	FMI	FMI 483
AETH 2λ, AE21	426	ECPL	ECPL 426
AETH 7λ, AE31	563	CAWAS	CAWAS 563
AETH white light, AE9	910101	MHD	MHD 910101
AETH white light, AE10	70010	MHOP	MHOP 70010
AETH 7λ, AE31	337	PSI	PSI 337
MAAP	032	IFT	IFT 32
MAAP	049	FMI	FMI 49
MAAP	050	IZANA	IZANA 50
MAAP	30	MHD	MHD 30
MAAP	1A	DLR	DLR 01A
MAAP	13	MHOP	MHOP 13
MAAP	39	MMS	MMS 39

2 Experimental Setup

To ease the understanding of the formulas in Table 2.1 often used abbreviation are given.

Table 2.1: Nomenclature

λ	Wavelength of light
σ_{ap}	Particle absorption coefficient
$\sigma_{sp,\lambda}$	Particle scattering coefficient at wavelength λ (λ=450,550 or 700 nm). The particle scattering coefficient is measured using the Nephelometer. The values are <u>not</u> corrected for the truncation error.
$\Delta\sigma_{ap,X}$	Unit to unit variability of instrument class X
SSA	Single scattering albedo : $SSA=\sigma_{sp}/(\sigma_{sp}+\sigma_{sp})$
R_{eff}	Effective radius. The effective radius is the 1^{st} moment of the number size distribution.
$Å_{sca}$	Ångstroem exponent for scattering
$Å_{abs}$	Ångstroem exponent for absorption
Subscripts	
ap	Particle absorption
sp	Particle scattering

2.1 Instruments

2.1.1 PSAP

The functional principle of the Particle Soot Absorption Photometer (model PSAP, Radiance Research, Seattle, WA) is described in Bond et al. (1999). The PSAP with the nominal wavelength 567 are referred as the *old* PSAP. In the *new* PSAP the light source was replace by a diode emitting light at a shorter wavelength of about 530 nm. In addition the opal glass plate between light source and particle filter was replaced by a diffusely scattering hemisphere. A further modification of PSAP led to the 3-wavelength PSAP (Virkkula et al., 2005). The optical wavelengths are approx. 467, 531, and 650 nm. The wavelengths of all PSAPs were checked using an optical spectrometer. The method and results are given in Chapter 3.3.

In the last years correction schemes were developed by Bond et al. (1999) (in the following referred as *Bond correction*) and Virkkula et al. (2005). Although the Bond correction was for the *old* PSAP type, we apply it to the other types of PSAPs at all wavelengths. With this approach we want to ease the inter-comparison of all PSAPs, especially for an investigation of the unit to unit variability. Because of the fundamental approach for correcting the scattering artifact and the extrapolation of this correction to other wavelengths the correction scheme is described in more detail.

This correction method accounts for loading and scattering correction. A correction of the aerosol flow and correction of spot size has to be done. All these corrections were included in the correction method which is referred as *Bond correction*. These corrections were developed for the *old* PSAP having a nominal wavelength of 567 nm. However the applied scattering correction uses scattering coefficients at 550 nm, the center wavelength of the green channel of a nephelometer (TSI, model 3563). It is worth note that the scattering coefficients used for the Bond correction are not corrected for the so called truncation error (Anderson 1996, Heintzenberg 2006).

The change of the optical wavelength required to calculate scattering coefficients for the other wavelengths. The interpolation and extrapolation of scattering coefficients was done using the Ångstroem exponent α which is defined as: $\sigma_{sp}(\lambda_2) = \sigma_{sp}(\lambda_1) \cdot \left(\frac{\lambda_2}{\lambda_1} \right)^{\alpha}$.

With the scattering coefficients measured at 3 wavelengths an average Ångstroem exponent is calculated. The Ångstroem exponent was used for an interpolation of scattering coefficients for wavelengths between 450 nm and 700 nm.

The formula for the Bond correction is:

$$\sigma_{ap}(t) = \frac{A}{V} \ln\left(\frac{I(t-\Delta t)}{I(t)}\right) \cdot \frac{1}{1.317 \cdot \tau + 0.866} - 0.016 \cdot \sigma_{sp}.$$

In this formula A is the sample spot area, V the volume flow, τ the optical transmission and I(t) the measured intensity.

2.1.2 MAAP

The MAAP) (multi angle absorption photometer) was recently introduced and measures the radiation transmitted through and scattered back from a particle-loaded filter. A two stream radiative transfer model is used to minimize the cross sensitivity to particle scattering. A detailed description of this method can be found in Petzold (2004). The advantage of the MAAP compared to PSAP and Aethalometer is the in-situ correction of the scattering artifact.

2.1.3 Aethalometer

Four types of Aethalometers were used during the workshop. These were two white light Aethalometers (AE-9 and AE-10), one 2λ-Aethalometer (AE 21), and three 7λ-Aethalometers (AE-31). A more profound description of the Aethalometers can be found in the user manual (Hansen, 2005). To get the absorption coefficient the Aethalometer data need to be corrected.

The Aethalometer in principle measures the absorbance A(λ) ($A(\lambda) = -\ln\left(I(\lambda)/I(\lambda)_0\right)$). The Absorbance is related to the total BC (Black Carbon) concentration [BC] by $A(\lambda) = Sigma_{BC}(\lambda) \cdot [BC]$. The specific attenuation $Sigma_{BC}$ depends on the optical wavelength (see Table 2.2). It is worth to note, that the specific attenuation is not a physical constant. The specific attenuation coefficient is the product of the mass absorption coefficient and a correction function for the Aethalometer, which is needed to relate the temporal evolution of the absorbance to the physical absorption coefficient.

Table 2.3: Specific attenuation coefficient used for Aethalometer (Hansen (2005))

λ[nm]	$Sigma_{BC}$ [m^2/g]
370	39.5
470	31.1
520	28.1
590	24.8
660	22.2
880	16.6
950	15.4

The first correction of the Aethalometer data to absorption coefficients including a loading and scattering correction was reported by Weingartner(2003) for laboratory aerosols. Further correction methods were given by Arnott (2005) and Schmid (2006). The latter one is based on the method of Weingartner, but the resulting absorption coefficients are lower by about 30% for ambient aerosol. This discrepancy of calibrations has to be taken into account, when comparing absorption coefficients measured with Aethalometer and PSAP or MAAP.

2.1.4 Custom made photometers

Three custom made instruments were used during the workshop. Two of them are one wavelength PSAP like instruments (MISU, ITM). A short description of the home made PSAP from MISU and ITM and results are shown in a separate Chapter 4.7.

A third photometer is a spectral absorption photometer (SOAP) with a transmission and a reflection channel. The spectral range is from 250 to 800 with 25 nm optical resolution. The reflection channel will be used for a correction of the scattering artifact. The photometer is still not fully characterized and calibrated. Therefore only raw data (no loading and scattering correction) from the transmission channel are shown. This photometer makes use of the same particle filter as the PSASP. Also the ratio of flow rate and spot size is similar to PSAP in order to make these instruments more comparable.

2.1.5 Photoacoustic Spectrometer

A photoacoustic spectrometer was intended to be the reference instrument for measuring the absorption coefficient. Unfortunately the values are not plausible. Values of the PAS will not be used for the data evaluation.

2.1.6 Instrument classification

In order to ease the data evaluation we introduce a classification based on instrument type and wavelength.

Instrument classes:

MAAP: MAAPs with wavelengths between 636 and 638 nm (all MAAPs)

PSAP460: PSAP with wavelengths between 455 and 465 nm (FMI 90A [blue channel], NOAA 90B [blue channel])

PSAP530: PSAP with wavelengths between 522 and 531 nm (FMI 90A [green channel], NOAA 90B [green channel], IFT 71)

PSAP650: PSAP with wavelengths between 650 and 465 nm (FMI 90A [red channel], NOAA 90B [red channel])

PSAP570: PSAP with wavelengths between 550 and 585 nm (IFT 20A, IFT 20B, ECPL 48, [NOAA 13 is not included because of its height noise level])

Aeth370: Aethalometers with wavelengths between 376 and 377 nm (PSI 337, FMI 426, CAWAS 563, ECPL 426)

Aeth470: Aethalometers with wavelengths between 470 and 476 nm (PSI 337, FMI 426, CAWAS 563)

Aeth520: Aethalometers with wavelengths between 518 and 530 nm (PSI 337, FMI 426, CAWAS 563)

Aeth590: Aethalometers with wavelengths between 592 and 597 nm (PSI 337, FMI 426, CAWAS 563)

Aeth650: Aethalometers with wavelengths between 649 and 657 nm (PSI 337, FMI 426, CAWAS 563)

Aeth850: Aethalometers with wavelengths between 853 and 868 nm (PSI 337, FMI 426, CAWAS 563, ECLP 426)

Aeth940: Aethalometers with wavelengths between 940 and 942 nm (PSI 337, FMI 426, CAWAS 563)

2.2 Aerosol Sources

The aerosols used during the workshop were:

a) Ambient aerosol: Ambient aerosol was used for an inter-comparison of al instruments in parallel. For that experiment the air conditioning of the laboratory was switch off and the windows were opened.

b) Ammonium sulfate: For investigation of the cross sensitivity to purely scattering particles. Ammonium sulfate particles were generated using an atomizer.

c) Soot: The sensitivity to strongly absorbing particles was measured with soot (Printex 75) generated by an atomizer.

d) Mineral dust (china clay, quartzite, and hematite): Three types of mineral dust were used to quantify the sensitivity to a strongly scattering dust (china clay), a slightly absorbing dust (quartzite), and a strongly absorbing mineral dust (hematite). In a custom made dust generator particles were dispersed and super-micron particles were removed using a cyclone (aerodynamic cut-off diameter approx. 1 μm).

The aerosols b), c) and d) were fed into a mixing chamber (0.5 m^3) which was used as a buffering volume. The instruments were connected to the eight output ports of the mixing chamber. Two ports were used for additional aerosol characterization using a SMPS/APS for measuring the number size distribution and integrating nephelometer (TSI, model 3563) the scattering coefficient was measured using an integrating nephelometer for measuring the particle scattering coefficient.

2.3 Aerosol characterization

2.3.1 Nephelometer

The total scattering coefficient and the backscattering of the aerosols were measured using an integrating nephelometer (TSI, model 3563) three wavelengths (450 nm, 550 nm, and 700). Because of a truncation error the recorded total scattering and backscattering coefficients are smaller than the "real" scattering coefficients. A correction of this so called "truncation error" (Anderson et al., 1996) was not applied, because the scattering correction for the PSAP data according to Bond (1999) requires the uncorrected data from the nephelometer.

2.3.2 SMPS and APS

The particle number size distributions were recorded using a Scanning Mobility Particle Sizer (SMPS) in the size range 10 nm to 600 nm. Larger particles were recorded using an Aerodynamic Particle Sizer (APS, TSI model 3321). The APS measures the aerodynamic size spectrum, which has to be converted to a number size spectrum. This calculation requires the density ρ_p and the dynamic shape factor χ_p of the particles. The conversion was done using the following formula:

$$d_p = d_{aer} \cdot \sqrt{\chi_p / \rho_p}$$

For ambient aerosol and ammonium sulfate we assumed a particle density of 1.7 g/cm^3 and a dynamic shape factor of about unity. The other aerosols have a larger density but also the dynamic shape factor is larger than unity. The density and shape factor in most cases are unknown. When using a constant ratio of 1/1.7 for the ratio of shape factor and density we got a good fit to the number size distribution at a particle diameter around 500 nm. Figure 2.1 shows average particle number size distributions for the different aerosols during the workshop. With the assumption of a constant ratio of particle shape factor and density we got a smooth transition between the DMPS to the APS size distributions. The number size distribution for China Clay was corrupted because of fast fluctuations of the particle concentration during the SMPS scans.

2.3.3 Summary of aerosol characterization

Basic data for aerosol characterization are summarized in Table 2.4. The effective radius R_{eff} is used to estimate that particle radius, which has the strongest contribution to total scattering. The single scattering albedo was calculated using the absorption coefficients measured with PSAP (corrected according Bond (1999)) at 530 nm and MAAP at 637 nm scattering coefficients measured with the nephelometer. The scattering coefficients were interpolated to the wavelengths 530 and 637 nm. Furthermore the scattering coefficients were not corrected for the truncation error, therefore the given values for the single scattering albedo are slightly too low. Also given are the scattering and absorption coefficients at 550 nm and 637 nm respectively. Ångstroem coefficients for scattering and absorption were calculated using the 3λ-nephelometer and the 3λ-PSAP respectively.

The corresponding particle number size distributions are shown in Figure 2.1. The number size distribution is a composite of SMPS and APS spectra. The Spectral Optical Absorption Photometer (SOAP) was not calibrated, therefore no loading and scattering correction was applied. The raw absorption spectra are show in Figure 2.2

Because auf the limited number of output port of the mixing chamber and the limited aerosol flow, several measurements with the same aerosol and different subset of in-

struments was done. The absolute values of absorption and scattering coefficients may vary between the different runs. The values of the single scattering albedos, effective radii and the Ångstroem coefficients did not change for the same aerosol type.

Table 2.4: Properties of aerosol types used for inter-comparison. Given are average values; The maximum and minimum values are given in brackets.

aerosol type	*ambient air*	*sulfate*	*soot*	*dust quartzite*	*dust china clay*	*dust hematite*
R_{eff} [μm]	0.141	0.056	0.087	0.191	0.289	0.209
SSA at 637 nm	0.92 [0.90, 0.94]	1[1]	0.46 [0.45, 0.47]	0.986 [0.984, 0.989]	0.998 [0.996, 0.999]	0.891 [0.867, 0.947]
SSA at 530 nm	0.90 [0.89, 0.91]	1[1]	0.35 [0.33, 0.50]	0.962 [0.958, 0.964]	0.998 [0.995, 0.999]	0.528 [0.505, 0.552]
scattering coefficients at 550 nm [1/Mm]	97.37 [67.43, 16.61]	95.60 [89.72, 100.66]	56.75 [18.72, 90.37]	339.3 [215.4, 447.8]	3077.9 [696.8, 3880.4]	46.48 [14.10, 129.79]
absorption coefficients at 630 nm [1/Mm]	11.86 [8.38, 15.44]	0[1]	119.82 [76.68, 137.43]	3.77 [2.09, 2.57]	5.49 [1.70, 11.49]	6.59 [1.39, 19.09]
$Å_{sca}$(460 and 700 nm)	1.39 [1.25, 1.50]	2.57 [2.51, 2.64]	1.02 [0.96, 1.30]			
$Å_{abs}$(460 and 700 nm)	1.14	0[2]	0.80			

[1] The single scattering albedo of Ammonium Sulfate is defined to be unity. It is assumed that the absorption coefficient is zero.

	[1.09, 1.24]	[0.73, 0.86]			
$Å_{sca}$(460 and 550 nm)			0.68	0.12	-1.78
			[0.66, 0.70]	[0.06, 0.15]	[-2.41, -1.58]
$Å_{sca}$(560 and 700 nm)			1.18	0.44	-1.32
			[1.11, 1.25]	[0.36, 0.49]	[-1.48, -1.21]
$Å_{abs}$(460 and 530 nm)			3.77	4.60	1.38
			[3.54, 4.17]	[1.73, 8.94]	[1.31, 1.45]
$Å_{abs}$(530 and 650 nm)			4.81	2.54	7.88
			[4.57, 5.16]	[0.44, 11.68]	[7.57, 8.23]

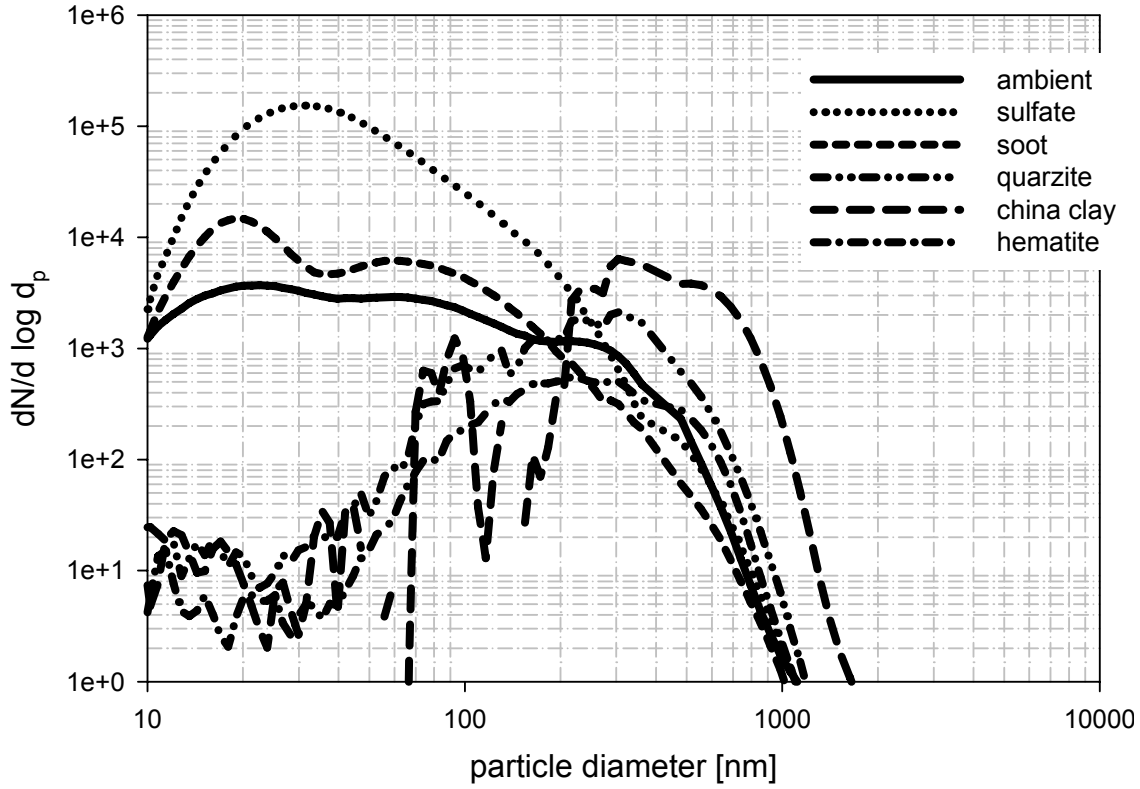

Figure 2.1: Average number size distribution of different types of aerosols. The number size distribution is a composite of SMPS and APS spectra. The output of the dust generator was not stable during the experiment using china clay.

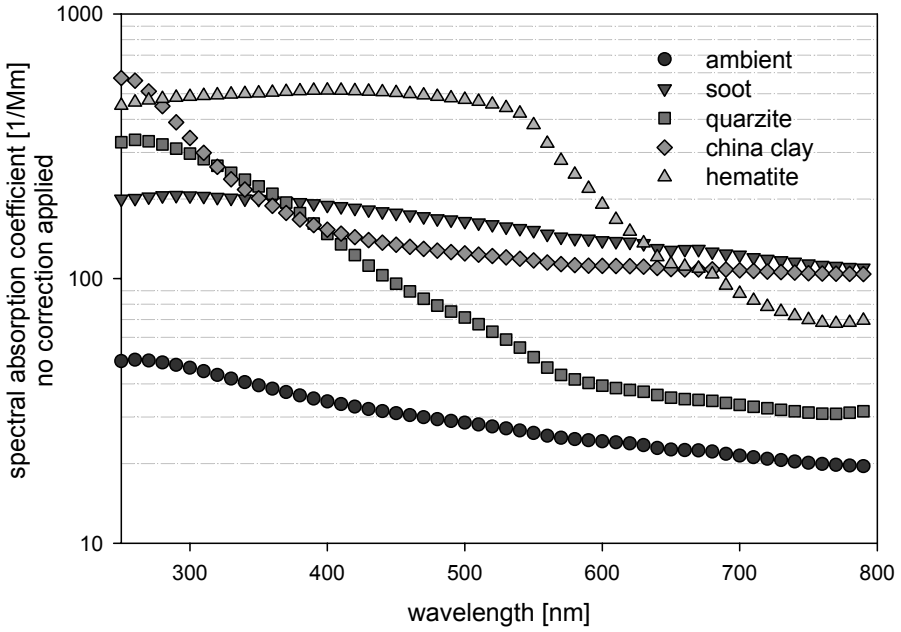

Figure 2.2: Absorption spectra measured with SOAP. No corrections for filter loading and scattering artifacts were applied.

3 Instrument characterization

3.1 Flow-rate

The flow rates of all instruments were calibrated using a primary flow standard. The Operating conditions of the instruments were room temperature and atmospheric air pressure. The absorption and scattering coefficients were corrected to STP (standard temperature and pressure) conditions. The standard temperature was set to room temperature. Thus the definition of STP was: T=20°C and P=1013.25 hPa.

PSAP: The PSAP measures the mass flow. This flow is corrected to STP conditions.

MAAP: Depending of the instrument settings the values are given for volume or mass flow at STD. The temperature used for STP correction can be change be the user.

Aethalometer: Depending of the instrument settings the values are given for volume or mass flow at STD. The temperature and pressure used for STP correction can be change be the user. The Aethalometer STP-settings for the three 7λ-Aethalometers were found to be [1013 hPa, 20°C], [1013 hPa, 25°C] and [1007 hPa, 20°C].

3.2 Spot sizes

The calculation of the absorption coefficient requires the "true" area of the sample spot. Variations from the nominal area given by the manufacturer have to be corrected. Therefore it is necessary to measure the area of each sample spot.

PSAP

The spot sizes for each PSAP were measured several times. The average diameter ranges from 5.62 to 4.77 mm. The maximum diameter of 5.62 mm was caused by a bad sealing (PSAP 48). The sealing was replaced afterwards. For calculating average sizes data from ECPL 48 were not included. The ratio of the measured and nominal sizes ranges from 1.06 to 0.87. A value of 1.06 results in an underestimation of 6% of the measured absorption coefficient if no spot size correction is applied. The average ratio of all PSAPs is 1.006, this means, that on average the spot size correction was smaller than 1% despite of the large unit to unit variation. The large unit to unit variation can be caused be variations of the filter itself or by the filter holder.

Table 3.1: Nominal and measured sample spot areas. Also given are the standard deviations for each instrument and the ratio of nominal and measured areas.

Instrument	*nominal diameter [mm]*	*measured diameter (average of 6 values) [mm]*	*standard deviation [mm]*	*ratio of measured and nominal area*
ECPL 48	5.1	5.62	0.12	1.21
FMI 90A	5.1	5.25	0.10	1.06
IFT 20A	5.1	5.45	0.08	1.14
IFT 20B	5.1	5.20	0.09	1.04
IFT 71	5.1	5.20	0.14	1.04
NOAA 90B	5.1	4.77	0.05	0.87
NOAA 13	5.1	4.92	0.07	0.93
average[2]	**5.1**	**5.13**	**0.09**	**1.006**

MAAP

No deviation from the nominal spot size can be observed.

Aethalometer

The spot sizes of the Aethalometers have to be discussed for each instrument separately. MHOP 70010, ECPL 426, and CAWAS 563 show a rather well defined spot area. The spot of CAWAS 563 is elongated, because this instrument was configured for "lower sensitivity".

The sample spots of FMI483 are overlapping. This problem can be solved by the settings of the Aethalometer. The error caused by overlapping spot can not be estimated.

PSI337 shows a more diffuse spot, which makes it difficult to determine the spot size.

The spot of MHD 910101 looks like a gray spot with a darker spot inside. The values reported by this instrument are not reliable.

The measured areas of the sample spots and the deviations from the nominal values are given in Table 3.2. On average the spot area of the Aethalometer are 8% lower than the spot sizes given by the manufacturer. This causes higher absorption coefficients of 8%.

[2] ECPL 48 was not included for calculating the average

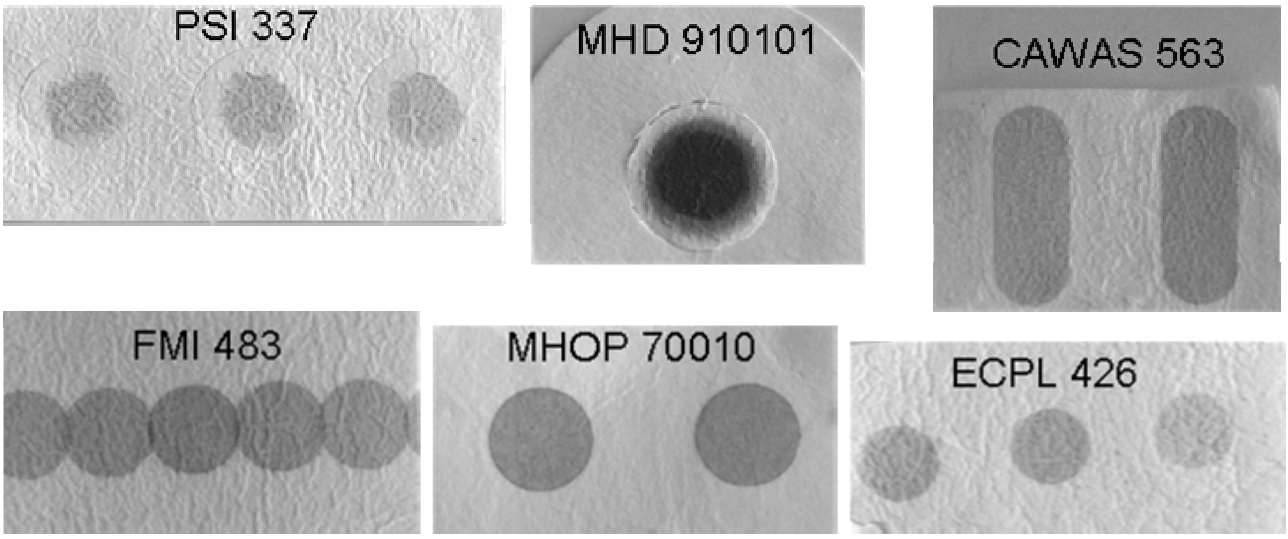

Figure 3.1: Photos of samples spot for the Aethalometers. The photos are not scaled.

Table 3.2: Nominal and measured spot areas for Aethalometers.

	nominal spot area [cm^2]	***measured spot area [cm^2]***	***ratio of measured and nominal area***
CAWAS 563	1.67	1.61	0.96
ECPL 426	0.5	0.49	0.97
MHOP 70010		0.92	-
PSI 337	0.5	0.46	0.91
FMI 483	0.5	0.43	0.85
MHD 910101		outer diameter 1.41 inner diameter 0.96	-
average			**0.92**

3.3 Operating Wavelength

The spectral emission of all MAAPs, PSAPs, and Aethalometers were measured using a fiber optic spectrometer (HR2000, Ocean Optics Inc.). The measured spectra are show in the Figures 3.2 to 3.6.

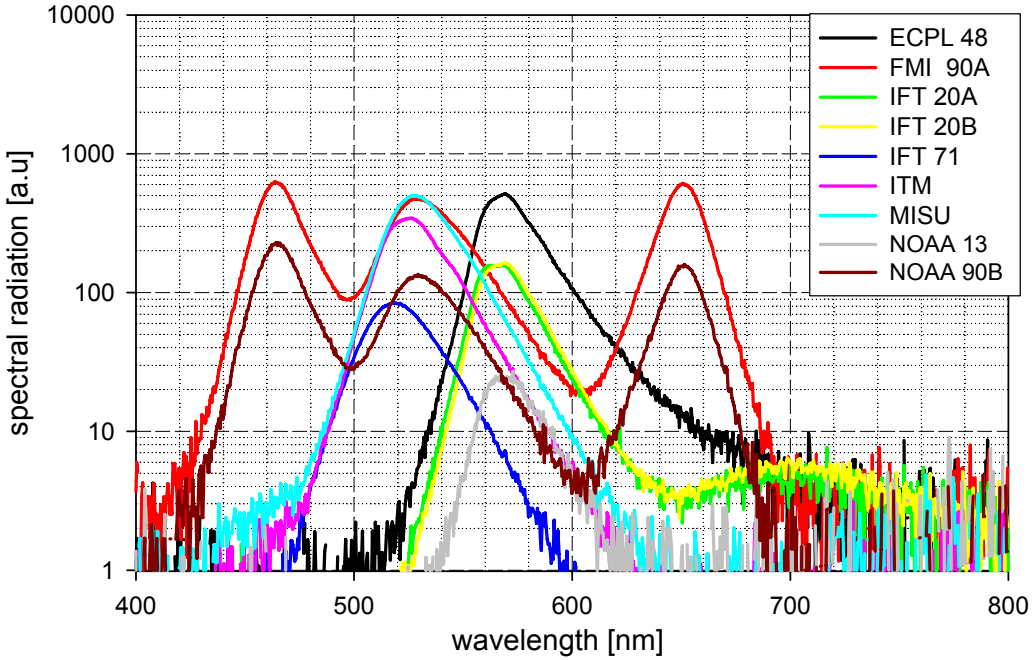

Figure 3.2: Spectral radiation of PSAPs.

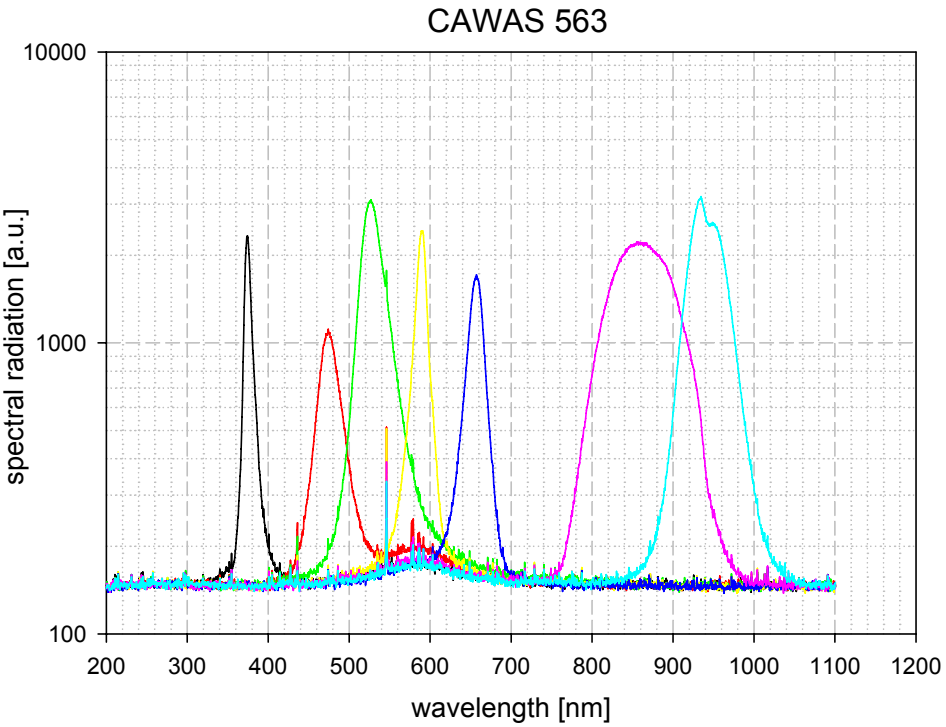

Figure 3.3: Spectral radiation of a 7λ-Aethalometer. The spectral radiation of the other 7λ-Aethalometer does not differ significantly from CAWAS 563. The shown spectra are not corrected for the background signal of the spectrometer and some scattered light from the outside.

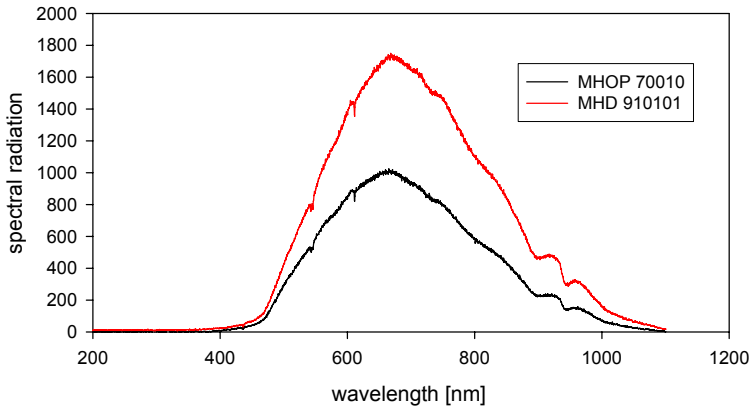

Figure 3.4: Spectral radiation white light Aethalometers (MHD 910101, MHOP 70010).

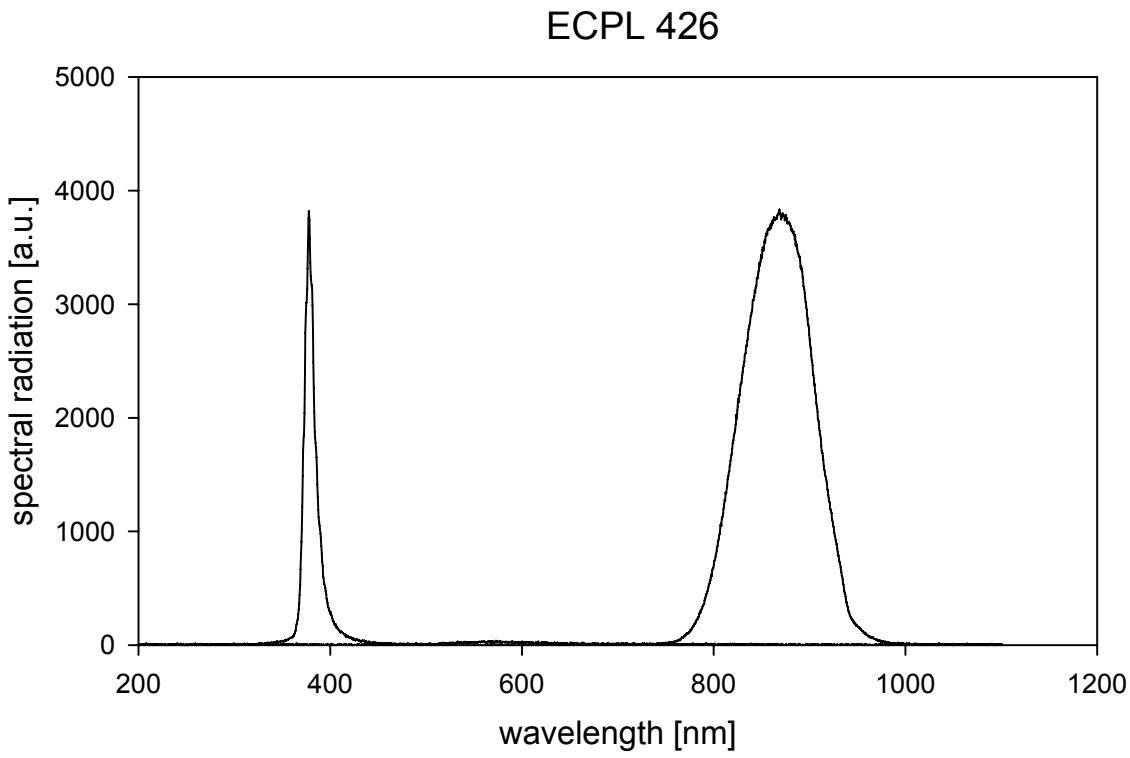

Figure 3.5 : Spectral radiation of the two 2λ-Aethalometer.

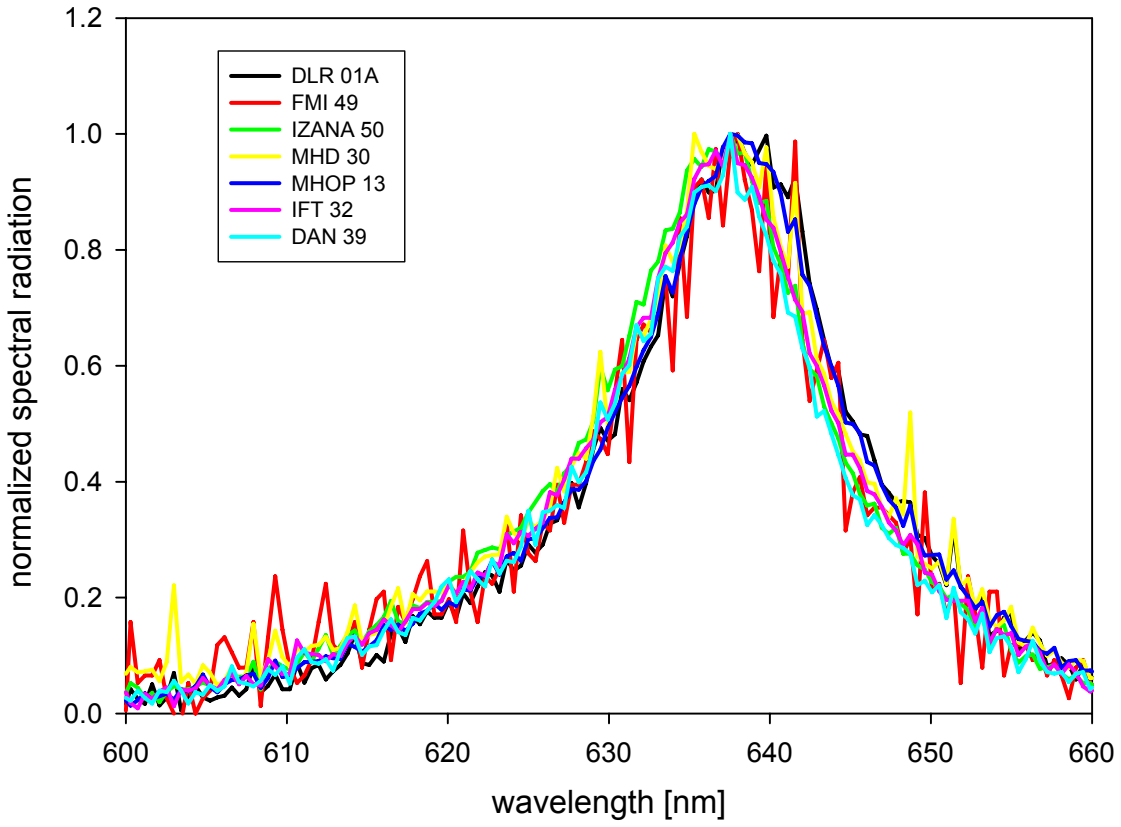

Figure 3.6: Spectral radiation of seven MAAPs. The optical intensity was very weak, because just some scattered light in the inlet of the MAAP was measured.

The spectral radiation was used to calculate an effective wavelength. Because of the non-symmetric spectra the first moment of the spectrum was used to calculate the effective wavelength using the formula:

$$\lambda_{eff} = \frac{\int_{\lambda_{start}}^{\lambda_{stop}} \lambda \cdot S(\lambda) \mathrm{d}\lambda}{\int_{\lambda_{start}}^{\lambda_{stop}} S(\lambda) \mathrm{d}\lambda}$$

where S(λ) is the spectral radiation. S(λ) was corrected for the spectrometer sensitivity and the spectral response of a typical silicon diode.

Table 3.3 gives the effective wavelengths for each instrument, the average wavelength of each instruments class, and the average deviation from the mean. The average deviation is defined as:

$$\Delta\lambda_{eff} = \left\langle \left| \lambda_{eff,i} - \left\langle \lambda_{eff,i} \right\rangle \right| \right\rangle$$

where $\langle\ \rangle$ is the average of the inner values

MAAP: The MAAP wavelengths are centered at 636.9 nm. This is contradictory to the wavelength of 670 nm which is given by the manufacturer! For a typical soot aerosol with Ångstroem exponent of 1.0 the absorption coefficient at 637 nm is 5% higher compared to the value at 670 nm.

Aethalometer: The IR wavelengths of the Aethalometer differ from the nominal values at 880 nm (860.2 nm measured) and 950 nm (940.9 nm measured). The other wavelengths are within ±6 nm to the nominal value.

PSAP: The nominal wavelength of the *old* PSAP is 565 nm. Because of a tail towards longer wavelengths, the effective wavelength is 584.7 nm. The *new* PSAP have an average wavelength of 529.6 nm. PSAP 71 has a significantly lower effective wavelength compared the other PSAPs.

Table 3.3: Measured effective wavelengths for each instrument, average of each instruments class, and average deviation.

Instrument	*nominal wave-length*								*average effective wavelength*	*standard deviation*
Aethalometer		**PSI 337**	**FMI 428**	**CAWAS 563**	**ECPL 426**					
	370 nm	376.2	375.8	374.9	378.1				**376.2**	0.9
	470 nm	472.1	470.9	475.4					**472.8**	1.7
	520 nm	529.4	518.1	528.7					**525.4**	4.9
	590 nm	596.5	592.2	589.2					**592.6**	2.6
	660 nm	649.7	655.3	656.5					**653.8**	2.8
	880 nm	853.1	858.6	861.8	867.3				**860.2**	4.4
	950 nm	940.5	941.2	940.9					**940.9**	0.2
MAAP		**DLR 01A**	**FMI 49**	**IZO 50**	**MHD 30**	**MHOP 13**				
	670 nm	637.8	636.9	636.2	636.9	637.6			**636.9**	0.5
PSAP		**ECPL 48**	**FMI 90A**	**IFT 20A**	**IFT 20B**	**IFT 71**	**ITM**	**MISU**		
	460 nm		467.4						**467.4**	-
	530 nm		531.2			522.1	530.7	534.1	**529.6**	4.5
	565 nm	579.9		584.4	589.4				**584.7**	3.9
	650 nm		649.8						**649.8**	-

4 Results of the inter-comparison measurements

Different experiments were performed to investigate the sensitivity of the absorption photometers to different aerosols and operating conditions. An experiment to investigate the dependence of the aerosol flow rate is described in Chapter 4.1. In Chapter 4.2 we give the noise levels of the instruments. The response to different types of aerosols is given in Chapters 4.2 to 4.6.

4.1 Aerosol flow-rate

The influence of the aerosol flow-rate was tested using 6 PSAPs, 2 Aethalometers, and 6 MAAPs. The flow rate of the PSAPs was varied from 0.4 lpm to 2.3 lpm, and the flow rate of MAAP was varied from 16.6 lpm to 8.3 lpm. The Aethalometer were operated with flow rates of 2.9 lpm and 5.6 lpm. This series of experiments was done with ambient air.

The Aethalometer 563 (low flow) was on average 16% higher than Aethalometer 428 (high flow). Considering the higher sensitivity of about 20% of Aethalometer 563 during the ambient air inter-comparison (Chapter 4.3), we can not find a dependence on the flow rate for Aethalometer.

The data from PSAP were corrected for scattering (Bond, 1999) and adjusted to 630 nm using the Ångstroem exponent. The ratios of the adjusted PSAP values and the average of 6 MAAPs versus the PSAP flow are shown in Figure 4.1. It is clearly visible that there is a dependence on the flow rate. For low flow (<0.5 lpm) and high flow (>2 lpm) the sensitivity is higher than for normal flow (~1 lpm). This result is in contrast Bond et al. (1999) were an inter-comparisons of different flow rates between 1 lpm and 2 lpm yields no differences exceeding the 6% instrument precision. An explanation for these differing results is missing.

A similar was done for MAAP (cf. Figure 4.1), where we compared individual MAAPs with different flow rates to the average value of all MAAPs. The result is, that there is no significant dependence on the flow-rate. The variability is within the 5% unit to unit variability.

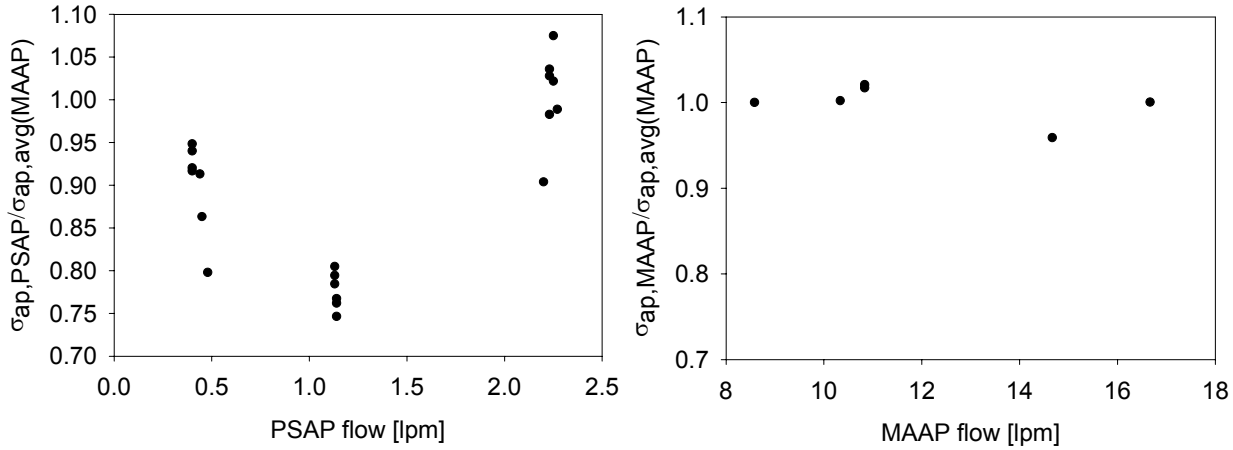

Figure 4.1: Left plot: Ratio of absorption coefficients measured with PSAP and the average of all MAAPs. The PSAP values were corrected according Bond (1999). All Values were adjusted to 630 nm using the Ångstroem formula. Right plot: Ratio of individual MAAPs with different flow rate and the average of all MAAPs.

4.2 Noise level/Filtered air

This experiment was dedicated to measure the noise level of the individual instruments using filtered air. The noise level is defined as the standard deviation of a time series of absorption coefficients using filtered air. The noise level was not measured for each instrument. Table 4.1 gives an overview of the results.

For MAAP the noise level was additionally estimated using data from an ambient air experiment (see Figure 4.2). At low aerosol concentration (σ_{ap}<4 Mm^{-1}) the average standard deviation of 6 MAAPs were 0.2 Mm^{-1}, and for the filtered air experiment the noise level was 0.08 Mm^{-1}

Table 4.1: Noise levels of individual instruments. Comments: a) The PSAP raw data corrected according to Bond; b) The Aethalometer raw data (concentration) were used to calculate the absorption coefficient using the recommended mass absorption coefficients. b2) Weingartner correction. c) Estimated from measurements with ambient aerosol at low concentrations. d) Measured using filtered air.

Instrument	*STD*	*time resolution*	*comment*

	[1/Mm]		
PSAP 13	1.06	1 min	a,d
PSAP 20B	0.33	1 min	a,d
PSAP 48	0.46	1 min	a,d
PSAP 71	0.30	1 min	a,d
PSAP 90B blue	0.06	1 min	a,d
PSAP 90B green	0.05	1 min	a,d
PSAP 90B red	0.05	1 min	a,d
Aeth. 426 (370nm)	0.42	3 min	b2,d
Aeth. 426 (880nm)	0.17	3 min	b2,d
Aeth. 70010 (880nm)	3.38	2 min	b,d
MAAP (average of six MAAPs)	~0.2	1 min	c
	<0.08	1 min	d

4.3 Sensitivity to the absorption of ambient air

During the ambient air test all instruments were operated in parallel in one laboratory. The air conditioning was switched and the windows of the laboratory were opened. A characterization of this aerosol is given in Chapter 2.2.

The unit to unit variability was calculated for MAAP, PSAP, and Aethalometer. The variability $\Delta\sigma_{ap}$ within one class of instruments is the defined as the spread (maximum-minimum) divided by the average of the individual instruments.

$$\Delta\sigma_{ap} = \frac{\max(\sigma_{ap,i}) - \min(\sigma_{ap,i})}{avg(\sigma_{ap,i})}$$

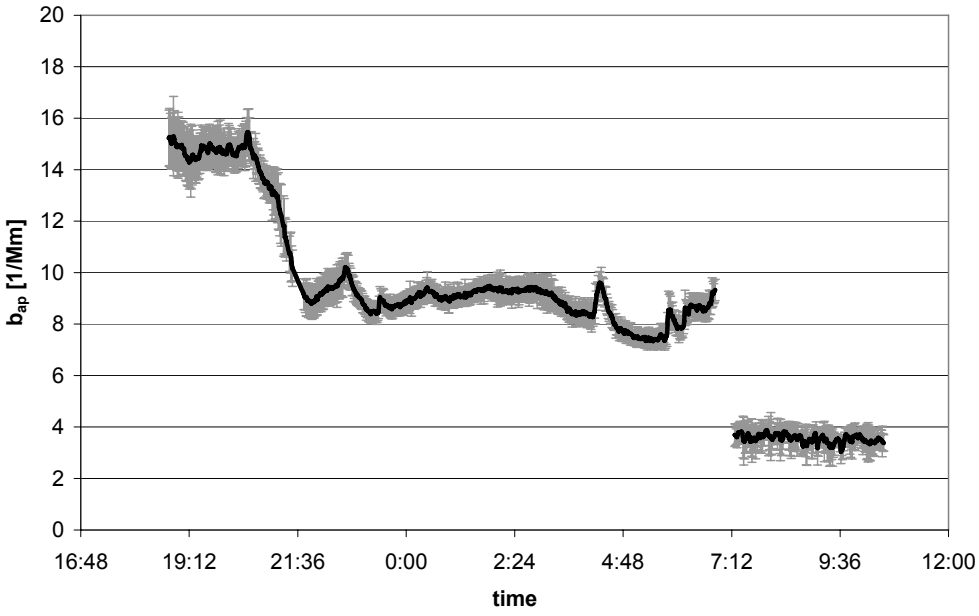

Figure 4.2: Time series of the average absorption coefficient measured with six MAAP. The error bars indicate unit to unit variability. At 7:00 the windows were closed and the air conditioning was switched on.

During the ambient air experiment the six MAAPs were compared. The average value and the unit to unit variability are shown in Figure 4.2. Because of the low unit to unit variability of 5% the MAAP is used as reference instrument for this workshop. In Table 4.2 the results of a linear regression of individual MAAP and the average of all MAAP are given.

Table 4.2: Linear regression (y=mx+b) of each MAAP vs. the average of six MAAPs.

MAAP	*m*	*y*	R^2
DLR 01A	0.958	0.084	0.997
13	1.016	-0.028	0.998
30	0.987	0.061	0.998
32	1.017	-0.063	0.995
49	1.014	0.018	0.998
50	1.009	-0.073	0.997

The MAAP 39 from MMS arrived when the workshop has ended. An inter-comparison with MAAP 032 using ambient air shows a regression line of $\sigma_{ap}(MAAP39)=0.95*\sigma_{ap}(MAAP32)+0.084$ with a regression coefficient of $R^2=0.98$.

MAAP 32 is 1.7% higher than the average of all MAAP. This shows that the values reported by MAAP 039 are within the range of uncertainties of the other MAAPs.

The variability of other instruments was much higher than for MAAP. The relative unit to unit variability is summarized in Table 4.3. Furthermore the relative sensitivity in relation to MAAP is given. All values were corrected to the wavelength 647 nm using the Ångstroem exponent. The Ångstroem exponent of 1.08 was calculated from a 3λ-PSAP.

Table 4.3: Relative sensitivity (compared to MAAP) and unit to unit variability. (a): Correction according to Bond (1999). The wavelength dependent absorption was taken into account using an Ångstroem exponent of 1.08. (b): Correction according to Weingartner (2003). The wavelength dependent absorption was taken into account using an Ångstroem exponent of 1.08. (c): Correction using a mass absorption coefficient of 20 m^2/g. No wavelength correction was applied.

instrument	*relative. sensitivity compared to MAAP at 637 nm*	*relative unit to unit variability [%]*	*corrections method*
MAAP 637 nm	1.00	5	-
PSAP 460 nm	0.81	16	(a)
PSAP 530 nm	0.79	24	(a)
PSAP 570 nm	0.86	32	(a)
PSAP 650 nm	0.81	9	(a)
Aeth. 370 nm	1.35	28	(b)
Aeth. 470 nm	1.25	28	(b)
Aeth. 520 nm	1.26	24	(b)
Aeth. 590 nm	1.31	18	(b)
Aeth. 660 nm	1.28	8	(b)
Aeth. 880 nm	1.26	24	(b)
Aeth. 950 nm	1.23	22	(b)
Aeth. S/N 70010	2.01	-	(c)

Aeth. S/N 91010	0.74	-	(c)

After correction of the wavelength dependence the relative sensitivity compared to MAAP were determined. The PSAP shows an average rel. sensitivity of 0.82. The "old" PSAPs show a slightly higher sensitivity at 580 nm.

The 7λ-Aethalometers have higher sensitivity of 1.28 compared to MAAP. Schmid (2006) presented a new Aethalometer correction. Using this correction the absorption coefficients are lower by a factor of 1.3 compared to Weingartner (2003). This new correction scheme agrees with the results of this experiment.

4.4 Soot

The relative sensitivity compared to MAAP was investigated using laboratory generated soot. Four experiments with different instrumentations were done. The results are summarized in Table 4.4.

Table 4.4: Relative sensitivity compared to MAAP. The absorption coefficients were corrected to 637 nm using the Ångstroem formula. The third column gives the correction method and the fourth column gives the Instrument ID, which was used as reference. a): Correction according to Bond (1999). The wavelength dependent absorption was taken into account using an Ångstroem exponent of 0.8. b): Correction according to Weingartner (2003). The wavelength dependent absorption was taken into account using an Ångstroem exponent of 0.8.

instrument	relative sensitivity	correction method	reference instrument
MAAP 032	0.95	-	MAAP 50
MAAP 050	-	-	no valid reference
MAAP 030	-	-	no valid reference
MAAP 13	-	-	no valid reference
MAAP 49	1.04	-	MAAP 50
PSAP 13 (not included in average)	1.17	a	MAAP 13
PSAP 20B	1.05	a	MAAP 13
PSAP 48	0.94	a	MAAP 32
PSAP 90B blue	0.84	a	MAAP 30
PSAP 90B green	0.83	a	MAAP 30
PSAP 90B red	0.80	a	MAAP 30

PSAP 71	1.10	a	MAAP 30,49
Aeth. 337, 370 nm	2.60	b	MAAP 50
Aeth. 337, 470 nm	2.13	b	MAAP 50
Aeth. 337, 520 nm	2.10	b	MAAP 50
Aeth. 337, 590 nm	2.11	b	MAAP 50
Aeth. 337, 660 nm	2.11	b	MAAP 50
Aeth. 337, 880 nm	2.15	b	MAAP 50
Aeth. 337, 950 nm	2.22	b	MAAP 50
Aeth. 426, 370 nm	3.07	b	MAAP 13 (might be incorrect)
Aeth. 426, 880 nm	3.29	b	MAAP 13 (might be incorrect)
Aeth. 483, 370 nm	-		
Aeth. 483, 470 nm	1.52	b	MAAP 50
Aeth. 483, 520 nm	1.49	b	MAAP 50
Aeth. 483, 590 nm	1.51	b	MAAP 50
Aeth. 483, 660 nm	1.53	b	MAAP 50
Aeth. 483, 880 nm	1.53	b	MAAP 50
Aeth. 483, 950 nm	-		
Average sensitivities			
PSAP	0.93		
7λ-Aethalometer (all wavelengths)	1.91		
7λ-Aethalometer (470 nm to 660 nm)	1.81		

4.5 Ammonium sulfate

The relative cross sensitivity to particle scattering was investigated using ammonium sulfate. The aerosol characterization is given in Chapter 2.3. The apparent absorption is the indicated absorption for purely scattering materials. The scattering was measured with a three wavelength nephelometer. The scattering coefficients were calculated for the individual wavelength of the absorption coefficient using the Ångstroem formula. Table 4.6 shows the relative apparent absorption (apparent absorption divided by the scattering coefficient).

Tabelle 4.5: Cross sensitivity to particle scattering. Given are the relative apparent absorption, the wavelength, and the correction method. a): Correction according to Bond (1999). The wavelength dependent scattering was taken into account using an Ångstroem exponent of 2.57 b): Correction using the mass absorption coefficients given in Table 2.3.

instrument	*relative apparent absorption [1/Mm]*	*wavelength [nm]*	*correction method*

MAAP 049	0.0069	637	
MAAP 01A	0.0065	637	
MAAP 050	0.0063	637	
MAAP 013	0.0062	637	
MAAP 030	0.0063	637	
MAAP 032	0.0051	637	
PSAP 20B	0.0172	585	a
PSAP 071	0.0089	530	a
PSAP 20A	0.0218	585	a
PSAP 90A_blue	0.0034	467	a
PSAP 90A_green	0.0042	530	a
PSAP 90A_red	0.0052	650	a
PSAP 90B_blue	0.0016	467	a
PSAP 90B_green	0.0042	530	a
PSAP 90B_red	0.0089	650	a
PSAP 013 (not included in avg.)	0.0312	585	a
PSAP 048	0.0164	585	a
Aeth. 483, 370 nm	0.0243	370	b
Aeth. 483, 470 nm	0.0348	470	b
Aeth. 483, 520 nm	0.0384	520	b
Aeth. 483, 590 nm	0.0453	590	b
Aeth. 483, 660 nm	0.0542	660	b
Aeth. 483, 880 nm	0.1039	880	b
Aeth. 483, 950 nm	0.1015	950	b
Aeth. 563, 370 nm	0.0278	370	b
Aeth. 563, 470 nm	0.0345	470	b
Aeth. 563, 520 nm	0.0571	520	b
Aeth. 563, 590 nm	0.0551	590	b
Aeth. 563, 660 nm	0.0447	660	b
Aeth. 563, 880 nm	0.1083	880	b
Aeth. 563, 950 nm	0.1171	950	b
Aeth. 426, 370 nm	0.0204	370	b
Aeth. 426, 880 nm	0.0850	880	b
Aeth. 337, 370 nm	0.0244	370	b
Aeth. 337, 470 nm	0.0339	470	b
Aeth. 337, 520 nm	0.0336	520	b
Aeth. 337, 590 nm	0.0419	590	b
Aeth. 337, 660 nm	0.0426	660	b
Aeth. 337, 880 nm	0.0518	880	b
Aeth. 337, 950 nm	0.0601	950	b
average cross sensitivity			
MAAP	0.0062		
PSAP (all wavelengths)	0.0092		
PSAP blue (467)	0.0025		
PSAP green(530)	0.0058		

PSAP green(585)	0.0185
PSAP red (650)	0.0070
Aethalometer (all wavelengths)	0.0539

The average cross sensitivity to particle scattering is lowest for MAAP with 0.63% of the scattering coefficient. The PSAP still shows an average cross sensitivity of 0.9% although the Bond correction was applied. The older PSAPs show at 580 a significantly larger cross sensitivity compared to the newer PSAPs. The Aethalometers has a cross sensitivity of about 5.4% in average. For PSAP and Aethalometer the cross sensitivity is higher for larger wavelengths.

4.6 Mineral dust

The measured absorption and scattering coefficients were normalized to the scattering coefficient at 550 nm. Figure 4.3 shows the absorption spectra and scattering spectra at three wavelengths measured with a 3λ-PSAP, MAAP, and the nephelometer. PSAP values were corrected according the Bond formula.

Quartzite and china clay are strongly scattering minerals. For china clay, what is nearly perfect white for the human eye, the indicated absorption is close to zero (0.2%, -1.0%, -1.3%). The indicated absorption is the remaining apparent absorption due to particle scattering. That means that the Bond formula overcorrects the scattering artifact for this mineral.

Hematite is a red iron oxide. At 460 nm hematite is strongly absorbing, whereas the absorption at 650 nm is very low.

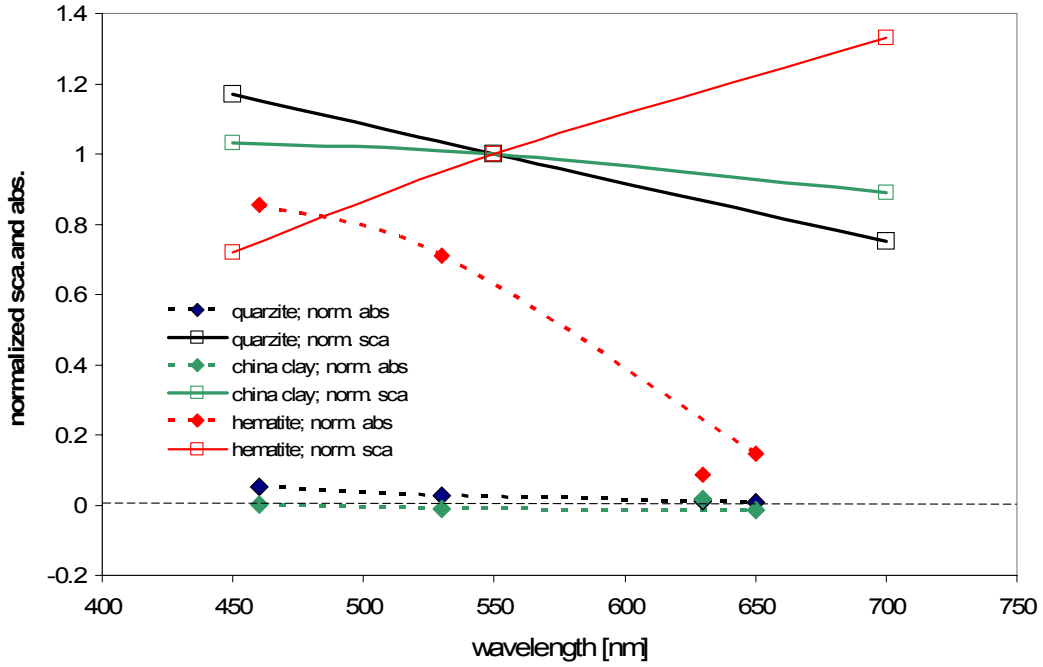

Figure 4.3: Normalized absorption and scattering coefficients for quartzite (black), china clay (green), and hematite (red). Values are normalized to the scattering coefficient at 550 nm.

4.7 Results of MISU and ITM PSAPs

The MISU and ITM PSAPs both measure in transmission and the ITM in addition measure the reflectance. In Figures 4.4 the reflectance and transmittance are shown. The transmittance and reflectance are defined by:

$$\mathrm{Tr}(t) = -\ln\left(\frac{I_T(t)}{I_T(t=0)}\right) \text{ and } \mathrm{Ref}(t) = -\ln\left(\frac{I_R(t)}{I_R(t=0)}\right).$$

It can be seen that both the reflectance and transmittance are increasing with time when sampling absorbing aerosol. White aerosols can lead to a negative transmittance as it can be seen for ammonium sulfate and china clay.

The reflectance for the ITM photometer is always higher than for the ITM photometer. The reasons are different ratios of spot size and sample flow. This measurement shows that a reflection channel can be used to differentiate between scattering and absorbing particles.

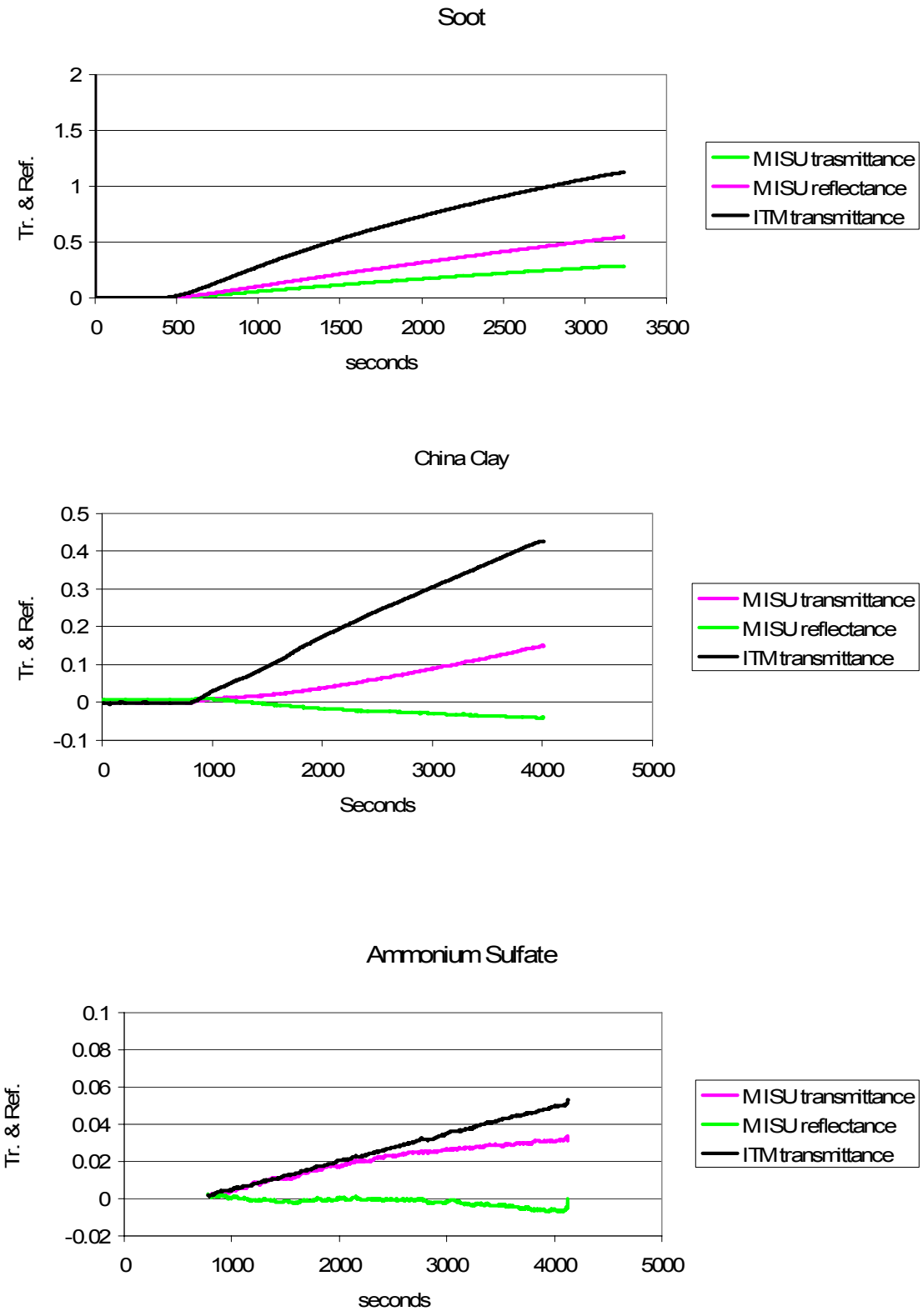

Figures 4.4: Transmittance and Reflectance for the MISU and ITM photometers.

4.8 Summary of experiments

The MAAP shows a unit to unit variability of 5% for absorption coefficients above 8 Mm^{-1} and a signal to noise ratio of 0.08 Mm^{-1} measured with filtered air with one minute integration time. The cross sensitivity to particle scattering is 0.6 %.

The Aethalometer has a noise level of about 0.42 and 0.17 at the wavelengths 370 and 880 nm respectively for an integration time of 3 minutes. The unit to unit variability is up to 28%. The relative sensitivity compared to MAAP is 1.28 for ambient aerosol and 1.91 for soot. The high sensitivity to soot might be an experimental error, because the variability of the different Aethalometers was about 50%. The average cross sensitivity to scattering particles is 5.4%.

Aethalometer has a higher sensitivity to ambient air and soot. Using the Schmid correction instead of the Weingartner correction, the relative sensitivity is 0.98 (compared to MAAP). The latter correction was derived from experiments using ambient aerosol. The unit to unit variability and the signal to noise ratio are much larger than for MAAP. The high unit to unit variability might be caused be the variations of the spot size.

The 1λ-PSAPs have an average signal to noise ratio of 0.36 Mm^{-1} whereas the 3λ-PSAPs have a much lower signal to noise ratio of about 0.053 Mm^{-1}. The unit to unit variability is 16%, 24%, and 9% for the three wavelengths of the 3λ-PSAP (blue, green, red) and the *new* 1λ-PSAP at 530 nm. The *old* PSAP at 580 nm have a unit to unit variability of 32%. This value might be caused be a wrongly determined spot sizes, because of rather diffuse sample spots. The sealing of PSAP 48 was replaced afterwards. The relative sensitivity compared to MAAP for ambient aerosol is 0.81 (460 nm), 0.79 (530 nm) and 0.81 (650 nm), and 0.86 (580 nm) whereas the latter value is for the *old* PSAPs. For soot the relative sensitivity is slightly higher with 0.93.

The unit to unit variability and the noise level of PSAP are lower than for Aethalometer and higher compared to MAAP. The sensitivity to absorption is lower compared to MAAP and Aethalometer. The cross sensitivity to scattering particles can clearly be seen although the bond correction was applied. For Ammonium sulfate the cross sensitivity to particle scattering is on average 0.92% although the Bond correction was applied. The old PSAP have the largest values of 1.8%. At the wavelengths 460, 530, and 650 nm the 3λ-PSAPs and the *new* PSAP have a cross sensitivity with 0.25%, 0.58% and 0.7%. In contrast to the ammonium sulfate experiment, measurement with the white mineral dust shows, that the Bond correction is capable of removing the scattering artifact. Beside the chemical composition and the shape of the particle, the main difference between these two aerosols is the effective radius. The radii are 0.056 μm and 0.289 μm for ammonium sulfate and china clay, respectively.

5 Discussion

The large unit to unit variability may be caused by several reasons. First there is the need for an accurate measurement of the sample flow and a well defined sample spot area. The problem with sample spot variability can be overcome by larger spot sizes, and a better sealing of the filter holder.

Beside technical improvements a better understanding of the optical radiative transfer of the particle-filter-system is needed. In case of the MAAP is can be seen that a radiative transfer model is a significant improvement.

The reasons for the different sensitivities to absorption and scattering are manifold. All the experiments for calibrating the instruments were done separately. Therefore different aerosols and different reference absorption measurements were used. In a recent study (Sheridan, 2005) the sensitivities of MAAP, Aethalometer, and PSAP were investigated simultaneously using a mixture of kerosene soot and ammonium sulfate. It was seen that the sensitivity of PSAP is lower compared to a reference measurement depending on the absorption level. For high absorption the slope of the regression line was 0.78. For lower levels ($\sigma_{ap} < 200$ Mm^{-1}) the regression line changes to 0.86 and for typical atmospheric levels the ($\sigma_{ap} < 25$ Mm^{-1}) the regression slope was ~ 1.02. This results show, that correction functions depend and many parameters. During the same study MAAP showed close agreement with a reference absorption measurement by extinction minus scattering (Petzold, 2005).

The sensitivity to scattering particles is still a not well understood problem. The method introduced by Bond (1999) is only a first order correction[3]. The dependence on the particle scattering was attributed to the total particle scattering (neglecting the truncation error of nephelometer). Till now a theoretical based model is missing which includes the particle backscattering in addition to the total particle scattering. The different cross sensitivities for ammonium sulfate and china clay suggest that also the particle size could play an important role. The problem to find a loading and scattering correction function for the Aethalometer is similar to PSAP.

---

[3] Bond (1999) "…Our approach does constitute … a first-order correction that can readily be applied to absorption measurements whenever simultaneous light scattering data are available…"

6 References

Anderson, T. L., et al., (1996). „Performance characteristics of a highsensitivity, three-wavelength, total scatter/backscatter nephelometer“, J. Atmos. Oceanic Technol., 13, 967-986, 1996.

Arnott, W. P., et al. (2005).“ Towards aerosol light-absorption measurements with a 7-wavelength aethalometer: Evaluation with a photoacoustic instrument and 3-wavelength nephelometer“, Aerosol Sci. Technol., 39, 17–29.

Bond, T. C., et al. (1999). "Calibration and intercomparison of filter-based measurements of visible light absorption by aerosols." Aerosol Sci. Technol. 30: 582-600.

Hansen, A.D.A (2005). “The Aethalometer”, Magee Scientific Company, Berkley, California, USA, http://www.mageesci.com/book/Aethalometer_book_2005.07.03.pdf

Heintzenberg, J.,et al., (2006) “Intercomparisons and aerosol calibrations of 12 commercial integrating nephelometers of three manufacturers” Journal of Atmospheric and Oceanic Technology 23 (7): 902-914

Petzold, A., et al., (2004). "Multi-angle absorption photometry - a new method for the measurement of aerosol light absorption and atmospheric black carbon." J. Aerosol Sci. 35: 421-441.

Petzold, A, et al.(2005).“Evaluation of Multiangle absorption Photometry for Measuring Aerosol Light Absorption”. Aerosol Sci. Technol., 39:40-51.

Schmid, O., et al., (2006).“Spectral light absorption by ambient aerosols influenced by biomass burning in the Amazon Basin. I: Comparison and field calibration of absorption measurement techniques.“ Atmos. Chem. Phys., 6, 3443–3462.

Sheridan, P.J., et al., (2005) “The Reno Aerosol Optics study: An Evaluation of Aerosol absorption Measurement Methods”, Aerosol Sci. Technol., 39, 1-16

Virkkula, A., et al. (2005).“ Modification, calibration and a field test of an instrument for measuring light absorption by particles“, Aerosol Sci. Technol., 39, 68–83.

Weingartner, et al. (2003). "Absorption of light by soot particles: Determination of the absorption coefficient by means of aethalometers." J. Aerosol Sci. 34: 1445-1463.